Wind Direction Fluctuation Analysis for Wind Turbines

Peng Guo[1], Si Chen[1], Jingchun Chu[2], David Infield[3]

(1. the School of Control and Computer Engineering, North China Electric Power University, Beijing, 102206, China.
2. Guodian United Power Technology Co., Ltd., Beijing, 100039, China.
3. the Institute of Energy and Environment within the Department of Electronic and Electrical Engineering, University of Strathclyde, Glasgow, G1 1XW, UK.)

Abstract

Fluctuations are a key characteristic of the wind resource. It is important to quantitatively analyze wind direction fluctuation due to its influence on the optimization of wind turbine yaw control. Based on wind resource data available from SCADA systems, a method is proposed to describe wind direction fluctuations in terms of fluctuation amplitude A and fluctuation duration T. A Weibull distribution is employed to fit the marginal probability density of both these two measures of wind direction fluctuations, and a mixed Copula used to connect the marginal distributions, establishing the joint probability density function. This representation has been verified through comparison with the real operating SCADA data. A set of indicators are extracted from the probability distribution which can accurately quantify the local wind direction fluctuation characteristics of a wind turbine. These indicators can be helpful in the optimization of the yaw control system parameters, facilitating an improvement in the power generating performance of the wind turbine.

Keywords: wind direction fluctuation, yaw system, Weibull distribution, mixed copula function, wind direction fluctuation indicators.

1. Introduction

The utilization of wind energy as an alternative source of power provides many advantages in terms of the environment and the economy. For the wind energy industry it is of central importance to maximize power generation through optimized control. The nature of the wind resource itself determines power generation performance.

Due to differences in terrain and the position of wakes, the wind resource experienced by individual wind turbines can differ significantly, even within the same wind farm. Features of the local wind resource that need to be considered include fluctuations in both wind speed and wind direction as well as the mean wind speed. These three dimensional turbulence characteristics affect the aerodynamics of the rotor and thus the turbine performance. It is thus important that this turbulence is properly quantified with the results used to guide in the control design and optimization.

The Weibull distribution is widely used to characterize the wind speed at a site, see for example references [1] to [5]. In [6], the authors use a Weibull function to fit the seasonal and annual wind speed distribution and from the associated wind power density conclude that for the site under study winter has the highest wind power density and autumn the lowest.

Different mathematical tools have been used to model wind resource fluctuations; for example [7] utilizes wavelet, autocorrelation and FFT techniques to analyze and model the fluctuating nature of wind speed. Alternatively, variogram functions can be used to quantify the rate of change of wind speed [8]. In [9], a combination of an Autoregressive Integrated Moving Average model and an Autoregressive Conditional Heteroskedasticity model (ARIMA-ARCH model) has been used to represent wind speed variations. Research presented in [10] demonstrates that a collection of deterministic models fitted separately to different frequency components of wind speed fluctuations can significantly increase modelling prediction accuracy. In [11],

three different classes of probability density functions are used to fit the wind speed fluctuation distributions.

The above researches are mainly focused on wind speed. Wind direction characteristics and associated fluctuations that are also important, and have a critical influence on the wind turbine yaw performance, have been little studied. [12] adopts a hybrid model combining a univariate ARIMA model with a Kalman Filter to predict the wind direction with the aim of optimizing the yaw control performance. In [13], a generalized advanced logistic distribution is used to model the dynamic characteristics of wind direction. In order to evaluate the influence of wind direction fluctuations on wind turbine power generation, [14] proposes a fluctuation coefficient of the wind direction together with a dynamic yaw coefficient based on yaw error (the angle between the wind direction and the nacelle direction).

Wind direction fluctuations directly influence the working condition of the wind turbine yaw system, [15] to [20]. When the wind direction changes significantly the yaw system will respond to rotate the nacelle to eliminate the yaw error and thus turn the rotor normal to the incident wind. This highlights the importance of wind direction statistics for tuning yaw system control parameters.

In this paper, a definition of wind direction fluctuation is proposed in section 2. The marginal distributions and joint distribution of the resulting measures of wind direction fluctuation are studied in section 3 and 4. In section 5, the relationship between the probability distribution parameters and the characteristics of wind direction fluctuations is analyzed, and the probability distribution parameters are used to accurately quantify the local wind direction fluctuation characteristics of wind turbines.

2. Method for defining wind direction fluctuation

The wind resource data used in this paper is the SCADA data from a wind farm in Anhui province, China. The yaw system for wind turbines usually uses a simple

dead-band control strategy with two control parameters: a yaw error threshold, and a yaw error duration threshold. When the wind turbine detects a yaw error angle larger than the yaw error threshold and this condition persists for longer than the duration threshold, the yaw system is activated to realign the nacelle with the wind. These two yaw control parameters for the wind turbines in the test wind farm are 10 degrees and 30 seconds respectively. The sampling rate of the SCADA data used in this paper is 1 second so as to adequately resolve the timescales associated with yaw control. Wind direction changes are random but it is difficult to directly derive the characteristics of the wind direction fluctuations from measured time series of wind direction. In this paper a quantitative approach is proposed based on fluctuation amplitude and fluctuation duration.

2.1 Definition of wind direction fluctuation amplitude and fluctuation duration

For the test wind turbines, wind direction is measured by ultrasonic anemometers. They don't have move parts and can give more accurate wind direction measurement than the mechanical vane anemometers. A wind direction series of 40 seconds is shown in Fig.1. The wind direction varies between 0 and 360 degrees and is quite different from the wind speed which is a linear scale variable. Wind direction cannot be averaged in the normal manner and methods applied to wind speed fluctuations, such as [9], cannot be applied to wind direction. A new method for quantifying wind direction fluctuation is needed.

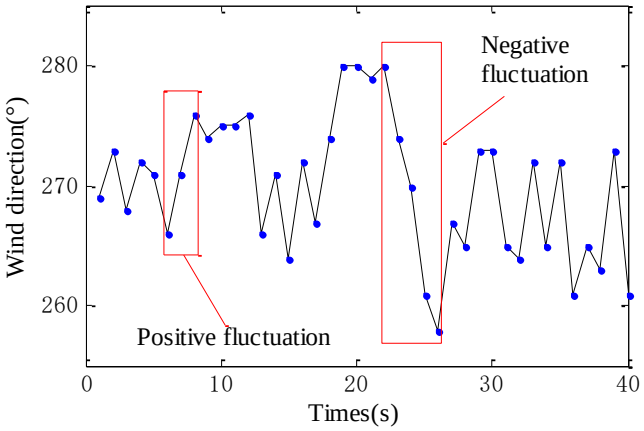

Fig. 1 Definition of positive and negative fluctuations

As in Fig. 1, a continuous monotonic increase of the wind direction angle is

defined as a positive fluctuation, and a continuous decrease defined as a negative fluctuation. Two parameters are associated with each wind direction fluctuation (both for positive and negative fluctuations), the fluctuation amplitude "A" and the fluctuation duration "T". The two parameters for the positive fluctuation in Fig.1 are respectively $A=10°$ and $T=2\text{s}$. And the two parameters for the negative fluctuation in Fig.1 are respectively $A=22°$ and $T=4\text{s}$. It should be noted that amplitudes are always positive irrespective of whether the fluctuation itself is positive or negative.

2.2 Two dimension wind direction fluctuation random variable (A, T)

For any wind direction time series, the wind direction fluctuation numbers for both positive and negative fluctuations are determined regardless of the size of the fluctuations according to the above definition. Fluctuation can thus been seen in terms of a two dimensional random variable (A, T). The properties of this random variable are not only related to individual random variables A and T, but also to the dependence between them.

The probability distribution function of the random variable (A, T) is defined as follows:

$$F(A,T)=P\left\{\left(X\le A\right)\bigcap\left(Y\le T\right)\right\}=P\left(X\le A,Y\le T\right) \tag{1}$$

where $A\in\left\{1°,2°,3°,\cdots\right\}$, and $T\in\left\{1\text{s},2\text{s},3\text{s},\cdots\right\}$.

All possible values for the discrete random variable (A, T) are $(a_i,t_j),i,j=1,2,\cdots,$ $a_i\in\left\{1°,2°,3°,\cdots\right\}$, $t_j\in\left\{1\text{s},2\text{s},3\text{s},\cdots\right\}$. The distribution law of discrete random variable (A, T) is $p_{ij}=\left\{A=a_i,T=t_j\right\}$.

An example distribution of the two dimensional discrete random variable (A, T) for wind turbine A03 is shown in Fig. 2 where small fluctuations (as defined below) have been ignored.

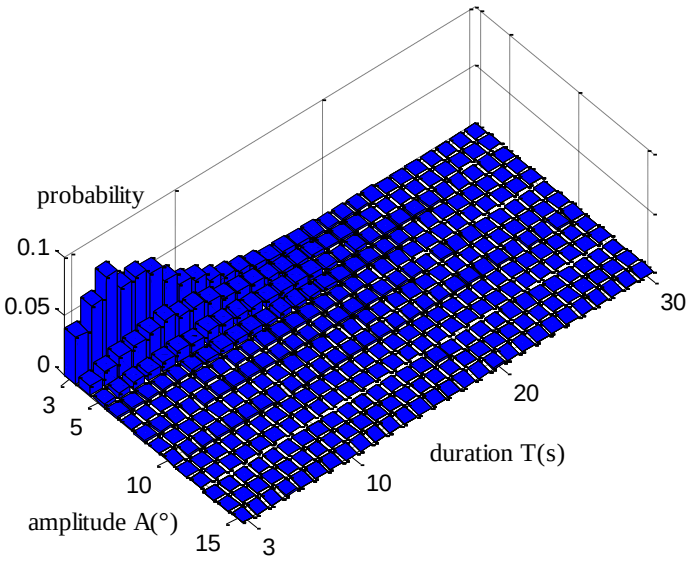

Fig.2 Distribution of random variable (A, T)

When the wind direction fluctuation amplitude is small ($A \le 2°$) or the fluctuation duration is short ($T \le 2\text{s}$), the yaw system won't be activated and the impact on wind energy capture will be insignificant (for example, when the yaw error is $\theta = 2°$, the power loss is approximately $\left[1-\cos^3(\theta)\right]\times 100\% \approx 0.183\%$). Therefore, Fig.2 only presents data where $A > 2°$ and $T > 2\text{s}$.

3. Marginal distribution probability density function (PDF) of the wind direction random variables A and T

Different geographical location and terrain of wind turbines will lead to different local wind direction fluctuation characteristics. Fig. 3 shows the geographical location and topography of each wind turbine in the test wind farm, and Fig. 4 is the contour map of the test wind farm.

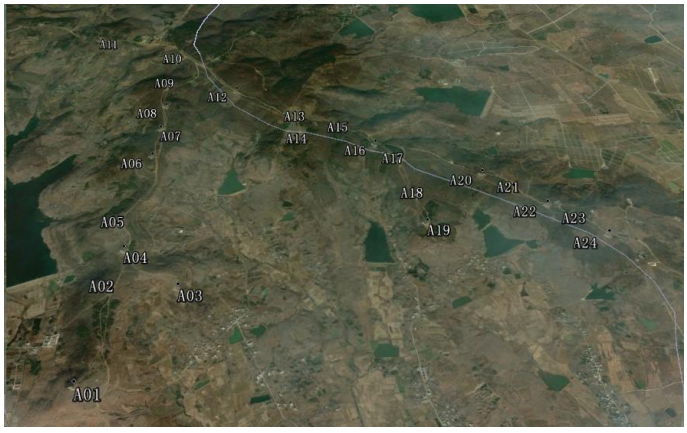

Fig. 3 Geographical location of each wind turbine

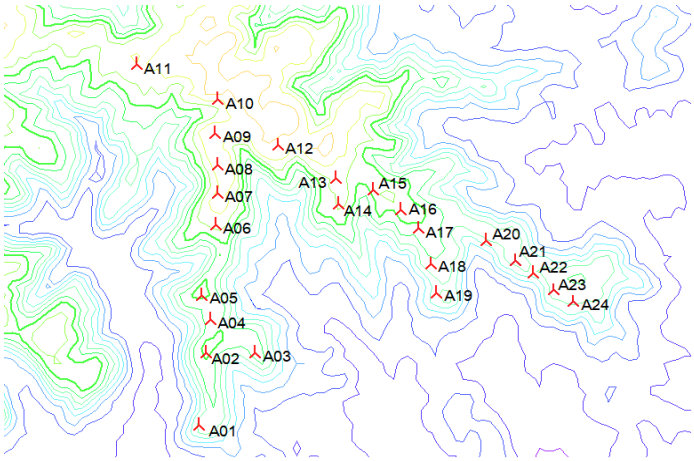

Fig. 4 Contour map of the test wind farm

Obviously, A03 is located on the leeward slope with hills on the northwest. In March, when the northwest wind prevails, because A03 has obvious terrain shelter in the dominant wind direction, the air flow accelerates on the windward slope of the hills in the northwest, while the wind speed decreases and the wind shear increases on the leeward side where A03 is located, resulting in poor local wind direction stability of A03. A09 is located at the top of the mountain, with open surrounding terrain and no obvious terrain shelter, so the wind direction of A09 is stable. Therefore, A03 and A09 are selected to respectively represent the wind turbines with unstable wind direction and the wind turbines with stable wind direction for analysis.

In order to obtain the joint probability distribution of the two dimensional wind direction random variable (A, T) in parametric form, the marginal distributions should first be studied. Wind direction data from 01/03/2015 to 08/03/2015 for two wind turbines A03 and A09 in the test wind farm were selected for comparative statistical analysis.

These two wind turbines are of same model (2 MW direct-drive turbines). The random variable (A, T) for the two wind turbines are calculated according to the definition of wind direction fluctuations in Section 2.1. After data has been filtered to remove points with $A \le 2°$ or $T \le 2\text{s}$, two sets of wind direction fluctuations for turbines A03 and A09 are obtained.

3.1 Marginal distribution probability histograms of the random variables A and T

Marginal probability density distributions of the wind direction random variables A and T for turbines A03 and A09 have been calculated. Fig. 5 and Fig. 6 are

respectively the histograms of the marginal probability distributions for fluctuation amplitude A and fluctuation duration T for the two test wind turbines.

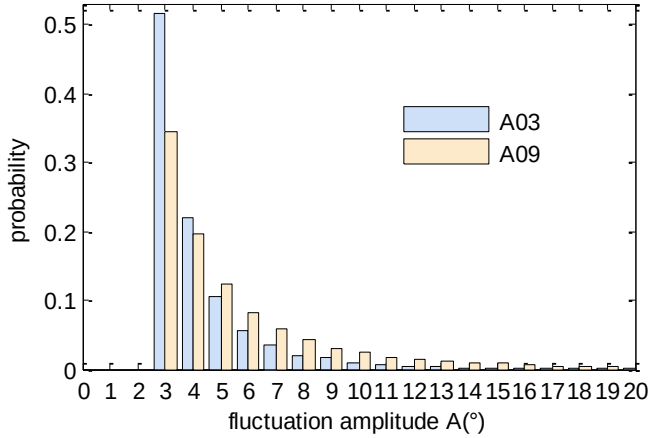

Fig. 5 Marginal distribution histogram of fluctuation amplitude A

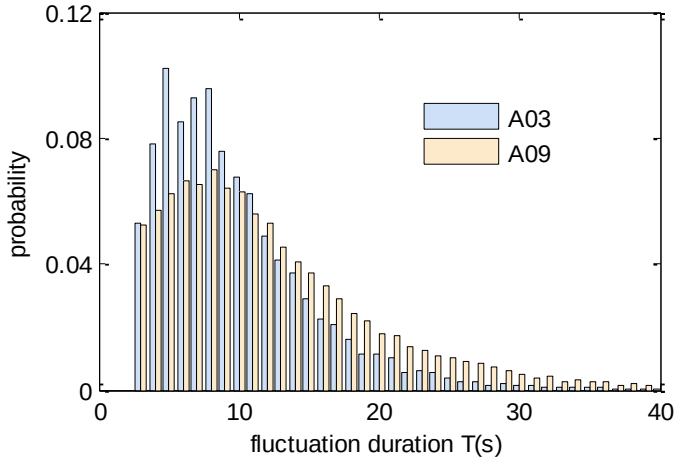

Fig. 6 Marginal distribution histogram of fluctuation duration T

From Figs. 5 and 6, it is clear that the data at A03 is quite different from that at A09. For A03, the probability of small fluctuation amplitude (A) and short fluctuation duration (T) is obviously higher than that of A09. That's to say, the wind direction at A03 tends to be more changeable and unstable compared with A09. On the contrary, for A09, the probability for wind direction fluctuations with long duration time is significantly higher than that of A03 indicating a higher probability for stable wind direction.

3.2 Marginal PDF fitting with Weibull distribution

In order to extract parametric distribution characteristics from the marginal distribution data for fluctuation amplitude A and fluctuation duration T, the Weibull distribution with displacement has been used.

The Weibull distribution with offset/displacement is as follows:

$$f(x)=\begin{cases}\dfrac{\beta}{\alpha}\left(\dfrac{x-m}{\alpha}\right)^{\beta-1} e^{-\left(\frac{x-m}{\alpha}\right)^{\beta}}, x\geq m\\ 0, x<m\end{cases} \tag{2}$$

where α is the scale parameter, β is the shape parameter, and m is the length of the displacement.

Least Square method is used to estimate the Weibull distribution parameters [4]. The parameters of fitted Weibull distribution for the fluctuation amplitude A are shown in Table I.

TABLE I Parameters of marginal distribution fitting for fluctuation amplitude A

	scale parameter α_A	shape parameter β_A	displacement m
A03	1.559	0.99	2
A09	2.801	0.96	2

The Weibull marginal distribution PDFs for the fluctuation amplitude A of A03 and A09 are shown in Fig. 7.

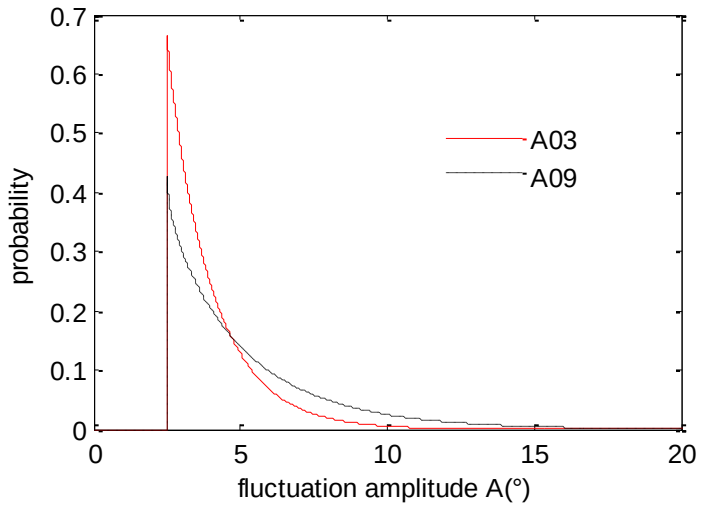

Fig. 7 Weibull distribution fitting for fluctuation amplitude A

The Weibull parameters for the fluctuation duration T are shown in Table II.

TABLE II Parameters of marginal distribution fitting for fluctuation duration T

	scale parameter α_T	shape parameter β_T	displacement m
A03	7.900	1.37	2
A09	10.838	1.23	2

The fitted Weibull marginal distribution for fluctuation duration T of A03 and A09 are shown in Fig.8.

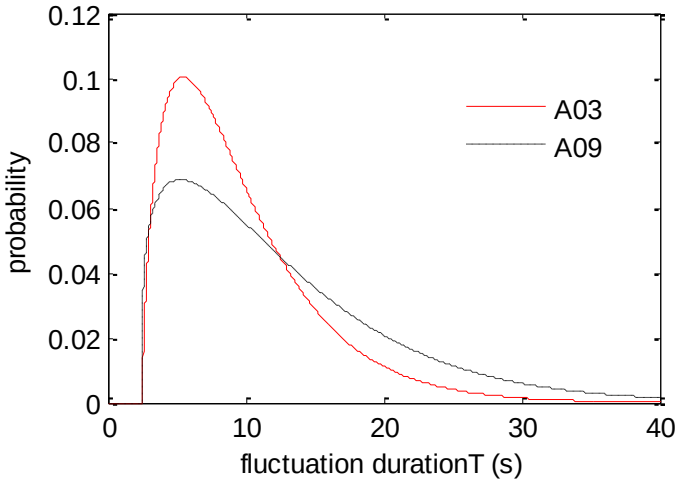

Fig. 8 Weibull distribution fitting for fluctuation duration T

The shape of the Weill distribution function is determined by the shape parameter. In Table I, shape parameters β_A are quite close to 1, and the two fitting curves in Fig. 7 are similar to the exponential distribution. In Table II, the shape parameters β_T are greater than 1, and the shapes of two fitting curves in Fig.8 are similar in shape to wind speed distributions with a well-defined maximum.

The Weibull scale parameter primarily determines the steepness of the fitting function. With a larger scale parameter α, probability density distribution will be flatter, and the tail of the fitting curve will have a higher density. It can be seen from Tables I and II that A09's scale parameters both for fluctuation amplitude A (α_A) and fluctuation duration T (α_T) are larger than that of A03. As a result, in Figs. 5 and 6, the fitting distribution functions for A09 exhibit a "fat tail" characteristic, while A03 has a "thin tail".

In summary, the characteristics of the wind direction fluctuations for both amplitude and duration can be satisfactorily represented by the Weibull scale parameters α_A and α_T respectively.

4 Joint distribution PDF of the wind direction random variable (A, T)

Copulas offer a means for expressing a joint distribution function in terms of the marginal distribution functions through a representation of the dependency between the random variables, [21-24].

The marginal distribution functions for the fluctuation amplitude A and the fluctuation duration T are as calculated in Section III. The task now is to identify a suitable copular function and so obtain the joint probability density function of the wind direction random variable (A, T).

Archimedean Copulas are widely used and include the Gumbel, Clayton and Frank Copulas, [25-28]. These Copulas together with a mixed Copula are considered as possible representations for random variable (A,T).

If u and v are the two marginal distribution PDFs for a two dimensional random variable, the Copular expressions are as follows:

(1) The Gumbel-Copula function

$$C_{\mathrm{G}}(u,v;\theta_{\mathrm{G}}) = \exp\left\{-\left[\left(-\ln(u)\right)^{\theta_{\mathrm{G}}} + \left(-\ln(v)\right)^{\theta_{\mathrm{G}}}\right]^{\frac{1}{\theta_{\mathrm{G}}}}\right\} \tag{3}$$

where, the dependent parameter $\theta_{\mathrm{G}} \in [1,+\infty)$. When $\theta_{\mathrm{G}} = 1$, the two variables are independent. When $\theta_{\mathrm{G}} \to \infty$, the two variables tend to complete dependence.

(2) The Clayton-Copula function

$$C_{\mathrm{cl}}(u,v;\theta_{\mathrm{cl}}) = Max\left(\left(u^{-\theta_{\mathrm{cl}}} + v^{-\theta_{\mathrm{cl}}} - 1\right)^{\frac{1}{\theta_{\mathrm{cl}}}}, 0\right) \tag{4}$$

where, the dependent parameter $\theta_{\mathrm{cl}} \in [-1,0) \bigcup (0,+\infty)$.

(3) The Frank-Copula function

$$C_{\mathrm{F}}(u,v;\theta_{\mathrm{F}}) = -\frac{1}{\theta_{\mathrm{F}}}\ln\left(1 - \frac{\left(1-e^{-\theta_{\mathrm{F}}u}\right)\left(1-e^{-\theta_{\mathrm{F}}v}\right)}{\left(1-e^{-\theta_{\mathrm{F}}}\right)}\right) \tag{5}$$

where, the dependent parameter $\theta_{\mathrm{F}} \neq 0$. When $\theta_{\mathrm{F}} > 0$, it signifies a positive correlation and when $\theta_{\mathrm{F}} < 0$, a negative correlation.

(4) The Mixed Copula function

$$C_{\mathrm{Mix}}(u,v;\omega_1,\omega_2,\omega_3) = \omega_1 C_{\mathrm{G}}(u,v;\theta_{\mathrm{G}}) + \omega_2 C_{\mathrm{cl}}(u,v;\theta_{\mathrm{cl}}) + \omega_3 C_{\mathrm{F}}(u,v;\theta_{\mathrm{F}}) \tag{6}$$

where $\omega_1, \omega_2, \omega_3$ are weight coefficients that satisfy:

$$\begin{cases} \omega_1, \omega_2, \omega_3 \in [0,1] \\ \omega_1 + \omega_2 + \omega_3 = 1 \end{cases} \tag{7}$$

To estimate the parameters of the Copula models, multi-stage maximum likelihood estimation method is used. We consider the two marginal models and the Copula model separately. [29] gives details on the validity of this procedure.

For the joint distribution PDF, the following RMSE is used as a measure of goodness-of-fit:

$$RMSE = \left(\frac{1}{n} \sum_{i=1}^{n} \left(Pe_i - P_i \right)^2 \right)^{1/2} \tag{8}$$

where Pe_i is the empirical probability, and P_i is the theoretical probability of the Copula.

Table III lists the RMSEs for the different Copula functions considered.

TABLE III RMSEs of different Copulas for A03 and A09

	copula function	**RMSE**
A03	Gumbel-Copula	0.0222
	Clayton-Copula	0.0416
	Frank-Copula	0.0187
	Mixed Copula	**0.0083**
A09	Gumbel-Copula	0.0202
	Clayton-Copula	0.0973
	Frank-Copula	0.0039
	Mixed Copula	**0.0012**

The mixed copula function fitting results for A03 and A09 are shown as Figs. 9 and 10.

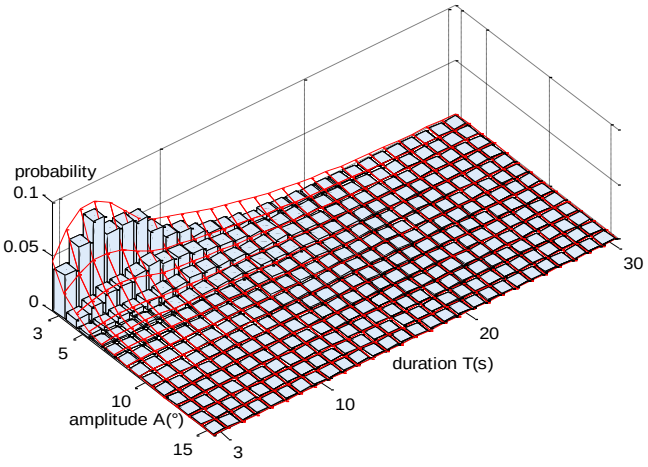

Fig. 9 Joint probability density function fitting result for A03

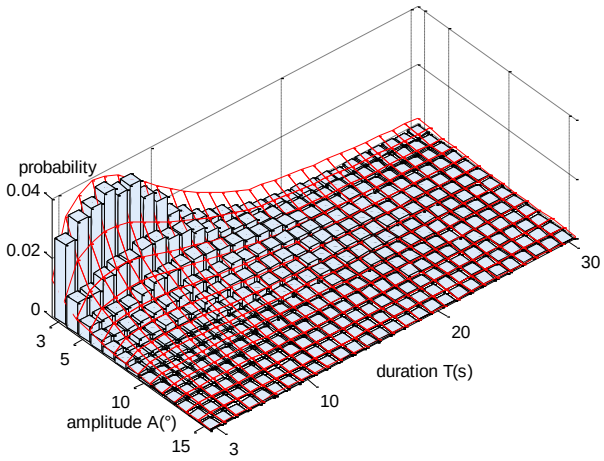

Fig. 10 Joint probability density function fitting result for A09

5. Wind direction fluctuation indicators

The joint distribution PDFs of the wind direction for A03 and A09 in section IV are shown together in Fig. 11 to allow comparison.

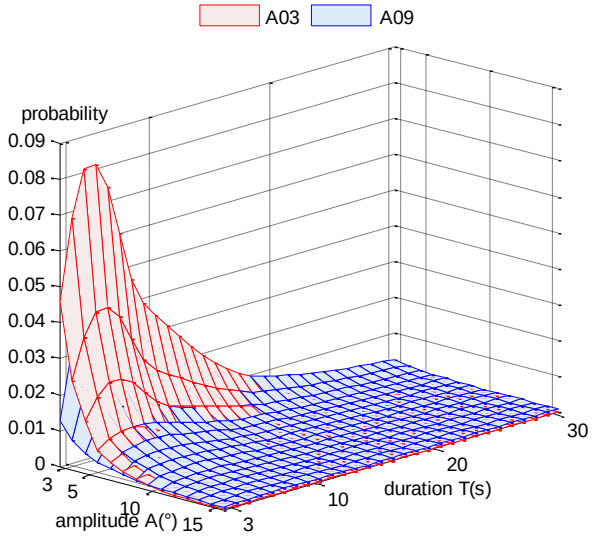

(a) View from front

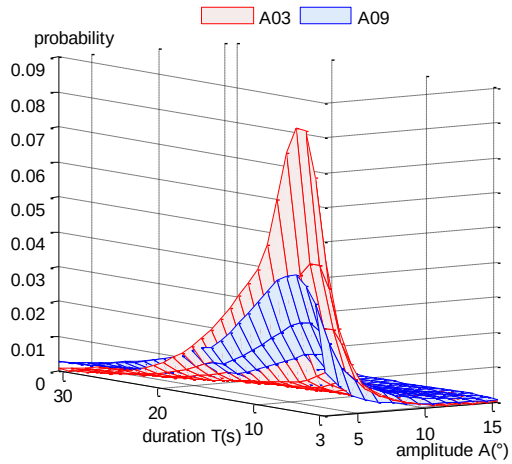

(b) View from behind

Fig. 11 Comparison of joint PDFs of A03 and A09

Careful examination of Fig.11 allows the following conclusions to be formulated:

(1) when the fluctuation amplitude A and the fluctuation duration T are small, the joint probability density of wind direction for A03 is obviously larger than that of the A09, which means that the A03 has more frequent wind direction fluctuations of small amplitude and duration than A09. These small transients are unlikely to activate the yaw system.

(2) For larger amplitudes and duration, the joint probability density for A09 exceeds that of A03. These significant wind direction fluctuations (changes) of large amplitude and long duration will activate the yaw system and potentially improve A09's power production.

In order to verify this analysis, statistics derived from the actual operation data for turbines A03 and A09 over the period 01/03/2015 to 08/03/2015 are shown in Table IV. During this time, both wind turbines ran normally without stopping.

TABLE IV Power generation and yaw statistics

Wind turbine	A03	A09
Average wind speed (m/s)	6.5	6.4
Yaw error threshold (°)	10	10
Yaw error duration threshold (s)	30	30
Yaw times	499	809
Power generation (kW·h)	115693	123320

Table IV shows that during this period, the average wind speed at the two turbines is quite similar. However, A09 yawed 809 times, which is significantly more than the 499 operations for A03, and the power generation of A09 was 6.6% greater than for A03. The operational data shows that the total number of wind direction fluctuations with large fluctuation amplitude and long fluctuation duration able to activate the yaw system is considerably higher for A09 than A03, and that A09 generates more power than A03. These results are consistent with the analysis provided for Fig.9. The usefulness of the mixed copula based joint distribution PDF for fitting wind direction fluctuations is confirmed.

In order to simply and directly quantify the stability of the local wind direction at wind turbines, a set of indicators that can accurately describe the fluctuation characteristics of local wind direction are extracted from the joint distribution PDF of the wind direction random variable (A,T). These indicators include:

(1) The scale parameter α_{A} in the Weibull marginal distribution PDF for the fluctuation amplitude A;

(2) The scale parameter α_{T} in the Weibull marginal distribution PDF for the fluctuation duration T;

(3) The probability of stable wind direction. With small fluctuation amplitude A (smaller than a predefined threshold EA) and long fluctuation duration T (larger than a predefined threshold ET), the wind direction can be defined to be stable. The probability of these stable wind directions is calculated from equation 9. At a wind turbine, a larger P_{stable} means that the local wind direction is more stable.

$$P_{\mathrm{stable}} = \int_0^{EA} \int_{ET}^{\infty} f(x,y)\,dxdy \tag{9}$$

where $f(x,y)$ is the mixed Copula joint distribution PDF of the wind direction random variable (A,T) in section 4. For the test wind turbines, the yaw system is activated when the yaw error angle exceeds 10° and this condition lasts for more than 30s. So it is reasonable to set $EA = 10°$, and $ET = 30\mathrm{s}$.

Table V shows the wind direction fluctuation indicators for A03 and A09.

TABLE V Wind direction fluctuation indicators for A03 and A09

indicators	A03	A09
α_{A}	1.559	2.801

α_T	7.900	10.838
P_{stable}	0.117	0.215

It can be observed from Table V that:

(1) The scale parameters α_A and α_T of A09 are larger than for A03;

(2) P_{stable} for A09 is much larger than P_{stable} for A03, which directly reflects the fact that the wind direction stabilities of A09 is greater than for A03.

In summary, the indicators of α_A, α_T and P_{stable} calculated from the wind turbine SCADA wind resource data can reflect the wind direction fluctuation characteristics of the wind turbine accurately and directly. With larger values of α_A, α_T and P_{stable}, the local wind direction at the wind turbine will be more stable.

6. Some Questions for Discussion

6.1 Two ~~other verification~~extra validation examples

For stronger and more credible validation, wind direction data from 01/03/2015 to 08/03/2015 of two more wind turbines A11 and A17,which are also in the test wind farm, were selected for comparative statistical analysis. The geographic position of A11 is similar to that of A09, it is located at the top of the mountain with no significant terrain shelter in the surrounding. While the geographic position of A17 is similar to that of A03, it is located at the leeward slope with hills on the northwest side.

The analysis results of A17 and A11 are shown in Table-VI~~VI~~:

TABLE ~~VI~~VI Wind direction fluctuation indicators for A17 and A11

indicators	A17	A11
α_A	1.812	3.443
α_T	8.363	11.207
P_{stable}	0.129	0.231

In Table ~~VI~~VI, the wind direction fluctuation indicators α_A、α_T and P_{stable} for A11 are all larger than for A17, which proves that the wind direction stability of A11 is better than A17. This is also consistent with the wind direction fluctuation characteristics that decided by the geographical location of A11 and A17. Therefore, it can be concluded that the three indicators proposed in this paper can effectively

measure the local wind direction fluctuation characteristics of wind turbines.

6.2 Wind direction fluctuation analysis of segmented wind speed

Different wind speeds may lead to different wind direction stability. In order to analyze the relationship between the wind speed and the wind direction fluctuation characteristics, the wind direction fluctuation random variable (A, T) were divided according to the low wind speed and the high wind speed. The low wind speed section refers to the range from 3 m/s to 7.5 m/s, and the high wind speed section refers to the range from 7.5 m/s to 12 m/s. Then the marginal probability distribution fitting and joint probability distribution fitting are carried out for the wind direction fluctuation random variable (A, T), and the indicators α_A, α_T and P_{stable} are calculated. Wind direction data from 01/03/2015 to 08/03/2015 for A03 and A09 in the test wind farm were selected for comparative statistical analysis once again. Table ~~Ⅶ~~VII shows the results.

TABLE ~~Ⅶ~~VII Wind direction fluctuation indicators of segmented wind speed for A03 and A09

indicators	3m/s~7.5m/s		7.5m/s~12m/s	
	A03	A09	A03	A09
α_A	1.372	1.783	1.947	3.120
α_T	6.487	8.028	8.116	12.319
P_{stable}	0.102	0.114	0.128	0.224

Some discoveries can be drawn from Table ~~Ⅶ~~VII:

(1) Whether in the high wind speed section or in the low wind speed section, α_A, α_T and P_{stable} for A03 are all smaller than for A09, which indicates that the wind direction stability is decided by the wind turbine geographic location instead of the wind speed.

(2) For A03, α_A, α_T and P_{stable} in the high wind speed section are all larger than in the low wind speed section; so does A09 wind turbine. Therefore, for the same wind turbine, the wind direction in the high wind speed section is more stable than in the low wind speed section.

(3) The difference between the three indicators for A03 and A09 in the high wind speed section is greater than that in the low wind speed section. This illustrates the greater the wind speed is, the more obvious the wind direction fluctuation

characteristic difference between different wind turbines are.

7. Conclusion

In this paper, wind direction fluctuation characteristics are analyzed based on wind resource data of four test wind turbines. This work supports the following conclusions:

(1) It is useful to define wind direction fluctuations in terms of a fluctuation amplitude, A and a fluctuation duration, T.

(2) The marginal distribution PDFs of A and T are well fitted by the Weibull distribution. A mixed Copula is provides an effective means to generate the joint distribution PDF of random variable (A,T). Operational data from two wind turbines demonstrates the accuracy of the mixed copula model.

(3) A set of indicators α_A, α_T and P_{stable} have been proposed that can quantify in a useful and effective manner local wind direction fluctuation characteristics and their stability with regard to wind turbine yaw performance. With wind resource data over an extended period of time and applying the methods developed in this paper, useful quantitative wind direction stability indictors can be calculated.

In future research, the yaw system control parameters for each individual wind turbine will be tuned using the wind direction stability indicators proposed in this paper. Firstly, it is necessary to establish a comprehensive economic benefit model of wind turbine based on the quantitative calculation of the fatigue loss of yaw bearing. This model should balance the restriction between the increase of power generation and the increase in yawing activity. Then, the wind direction stability indicators proposed in this paper are used to set the weight parameters in the model, and then the yaw control parameters (yaw error threshold and yaw error duration threshold) in the model are optimized. For the turbines with stable wind direction, such as A09 and A11, the yaw control parameters can be appropriately decreased to improve the sensitivity of the yaw system to wind direction changes, so as to obtain more wind energy at the cost of a slightly increase in yawing activity. On the other hand, for the wind turbines with poor wind direction stability such, as A03 and A17, the yaw parameters can be increased to reduce their sensitivity to frequently changing wind direction. Consequently, yaw operations can be drastically reduced at the cost of minimal loss of generation, but with the benefit of a considerable reduction of energy

used for yawing and fatigue damage to the yaw system. The yaw control parameters of each wind turbine in the wind farm are optimized to match the characteristics of local wind resources, so as to improve the economic performance of the wind farm as a whole.

References

[1] Wais P, “A review of Weibull functions in wind sector,” Renewable & Sustainable Energy Reviews, vol. 70, pp. 1099-1107, Apr. 2017.

[2] Usta I , Arik I , Yenilmez I , et al, “A new estimation approach based on moments for estimating Weibull parameters in wind power applications,” Energy Conversion & Management, vol. 164, pp. 570-578, May. 2018.

[3] Kaplan O , Temiz M, “A novel method based on Weibull distribution for short-term wind speed prediction,” International Journal of Hydrogen Energy, vol. 42, pp. 17793-17800, Jul. 2017.

[4] Wais P, “Two and three-parameter Weibull distribution in available wind power analysis,” Renewable Energy, vol. 103, pp. 15-29, Apr. 2017.

[5] Katinas V , Mantas Marčiukaitis, Giedrius Gecevičius, et al, “Statistical analysis of wind characteristics based on Weibull methods for estimation of power generation in Lithuania,” Renewable Energy, vol. 113, pp. 190-201, Dec. 2017.

[6] Devrim Y , Bilir L , Imir M , et al, “Seasonal and yearly wind speed distribution and wind power density analysis based on Weibull distribution function,” International Journal of Hydrogen Energy, vol. 40, no. 44, pp. 15301-15310, Nov. 2015.

[7] Zheng Q , Rehman S , Alam M M , et al, “Decomposition of wind speed fluctuations at different time scales,” Journal of Earth System Science, vol. 126, no. 3, pp. 36 , Mar. 2017.

[8] Liu J , Ren G , Wan J , et al, “Variogram time-series analysis of wind speed,” Renewable Energy, vol. 99, pp. 483-491, Dec. 2016.

[9] Masseran N, “Modeling the fluctuations of wind speed data by considering their mean and volatility effects,” Renewable & Sustainable Energy Reviews, vol. 54, pp. 777-784, Feb. 2016.

[10] Drisya G V , Asokan K , Kumar K S, “Diverse dynamical characteristics across the frequency spectrum of wind speed fluctuations,” Renewable Energy, vol. 119,

pp. 540-550, Apr. 2018.
[11] Calif R, “PDF models and synthetic model for the wind speed fluctuations based on the resolution of Langevin equation,” Applied Energy, vol. 99, pp. 173-182, Nov. 2012.
[12] Dongran S , Jian Y , Yao L , et al, “Wind direction prediction for yaw control of wind turbines,” International Journal of Control Automation & Systems, vol. 15, no. 4, pp. 1720-1728, Aug. 2017.
[13] Kaplya E V, “Generalization of the logistic distribution in the dynamic model of wind direction,” Izvestiya Atmospheric & Oceanic Physics, vol. 52, no. 7, pp. 760-767, Dec. 2016.
[14] Liu D , Long X , Cao J , et al, “Power fluctuation evaluation of large scale wind turbines based on SCADA data,” IET Renewable Power Generation, vol. 11, no. 4, pp. 395-402, May. 2017.
[15] Dai J , Yang X , Hu W , et al, “Effect investigation of yaw on wind turbine performance based on SCADA data,” Energy, vol. 149, pp. 684-696, Apr. 2017.
[16] KRAGH, Knud A , FLEMING, et al, “Increased Power Capture by Rotor Speed－Dependent Yaw Control of Wind Turbines,” Journal of Solar Energy Engineering, vol. 135, no. 3, pp. 1-7, Aug. 2013.
[17] Cortina G , Sharma V , Calaf M , et al, “Investigation of the incoming wind vector for improved wind turbine yaw-adjustment under different atmospheric and wind farm conditions,” Renewable Energy, vol. 101, pp. 376-386, Feb. 2017.
[18] Dongran Song, Xinyu Fan, Jian Yang, et al, “Power extraction efficiency optimization of horizontal-axis wind turbines through optimizing control parameters of yaw control systems using an intelligent method,” Applied Energy, vol. 224, pp. 267-279, Aug. 2017.
[19] Ouyang T , Kusiak A , He Y, “Predictive Model of Yaw Error in a Wind Turbine,” Energy, vol. 123, pp. 119-130, Mar. 2017.
[20] Choi D , Shin W , Ko K , et al, “Static and Dynamic Yaw Misalignments of Wind Turbines and Machine Learning Based Correction Methods Using LiDAR Data,” IEEE Transactions on Sustainable Energy, DOI 10.1109/TSTE.2018.2856919.
[21] Wang Y , Infield D G , Stephen B , et al, “Copula-based model for wind turbine power curve outlier rejection,” Wind Energy, vol. 17, no. 11, pp. 1677-1688, Nov. 2014.

[22] Pircalabu, Hvolby, Jung, et al, “Joint price and volumetric risk in wind power trading: A copula approach,” Energy Economics, vol. 62, pp. 139-154, Feb. 2017.
[23] Wang Z , Wang W , Liu C , et al, “Probabilistic Forecast for Multiple Wind Farms Based on Regular Vine Copulas,” IEEE Transactions on Power Systems, vol. 33, no. 1, pp. 578-589, Apr. 2017.
[24] Cao J, Yan Z, “Probabilistic optimal power flow considering dependences of wind speed among wind farms by pair-copula method,” International Journal of Electrical Power & Energy Systems, vol. 84, pp. 296-307, Jan. 2017.
[25] Konrad Furmańczyk, “Archimedean copulas with applications to estimation,” Statistical Methods & Applications, vol. 25, no. 2, pp. 269-283, Jun. 2016.
[26] Ahmed G , Wajdi H , Anis J, “Dependence between oil and commodities markets using time-varying Archimedean copulas and effectiveness of hedging strategies,” Journal of Applied Statistics, vol. 44, no. 9, pp. 1509-1542, Jun. 2016.
[27] Okhrin O , Tetereva A, “The Realized Hierarchical Archimedean Copula in Risk Modelling,” Econometrics, vol. 5, no. 2, pp. 1-31, Jun. 2017.
[28] Zuo D , Feng G , Zhang Z , et al, “Application of Archimedean copulas to the analysis of drought decadal variation in China,” Asia-Pacific Journal of Atmospheric Sciences, vol. 54, no. 2, pp. 125-143, Jun. 2018.
[29] Patton A.J., “Copula methods for forecasting multivariate time series,” Handbook of Ecnomic Forecasting, vol. 2, pp. 899-960, Dec.2013.